

NUMERICAL INTEGRATION OF CONSTRAINED HAMILTONIAN SYSTEMS USING DIRAC BRACKETS

WERNER M. SEILER

ABSTRACT. We study the numerical properties of the equations of motion of constrained systems obtained with Dirac brackets. This formulation is compared with one based on the extended Hamiltonian. As concrete examples a pendulum in Cartesian coordinates and a chain molecule are treated. We study the stability of the various formulations of the equations of motion based on a perturbed Hamiltonian state space form.

1. INTRODUCTION

The fundamental problem in the numerical integration of a constrained Hamiltonian system (or more generally of any differential algebraic equation [6]) is the drift off the constraint manifold. Geometrically seen, all dynamics happens on this manifold. Only it has a physical meaning; the ambient space is an artifact of the modeling. The dynamics is not well-defined outside the constraint manifold and can be modified, as long as it remains unchanged on the manifold.

Exact solutions are not affected by such modifications, as they live on the constraint manifold. But for numerical solutions any change can make a considerable difference. Due to the discretization error they typically leave the constraint manifold. The stability of the calculations depends decisively on the properties of the equations in the neighborhood of this manifold.

For Hamiltonian systems Dirac [9, 10] proposed modifications of the dynamics, although for other reasons. He introduced the total and the extended Hamiltonian, respectively, differing from the canonical one by a linear combination of constraint functions. On the constraint manifold both coincide and generate the same dynamics. But the extended Hamiltonian yields more stable equations of motion [20].

We study in this article the Hamilton-Dirac equations of motion derived with Dirac brackets [11]. This approach uses a modification of the symplectic structure of the phase space rather than of the Hamiltonian. We will show that it is equivalent to a simplification of the equations of motion derived with the extended Hamiltonian which was already mentioned in [20].

The basic idea behind Dirac brackets is the construction of an unconstrained Hamiltonian system (or underlying ordinary differential equation) which has the constraint functions as first integrals. For the special case of a regular system with imposed constraints the impetus-striction formalism [8, 22] achieves the same. In

1991 *Mathematics Subject Classification*. Primary 65L05, 70H05; Secondary 70-08.

Key words and phrases. Constrained Hamiltonian systems, Dirac brackets, stability, numerical integration.

This work was supported by Deutsche Forschungsgemeinschaft.

©0000 American Mathematical Society
0025-5718/00 \$1.00 + \$.25 per page

contrast, most index reduction techniques for general differential algebraic equations do not preserve the Hamiltonian structure of the system.

We will furthermore introduce a Hamiltonian version of the perturbation method of Alishenas [1, 2] to analyze the drift off the constraint manifold in some detail. This includes the introduction of a perturbed Hamiltonian state space form. Our approach will allow us to explain theoretically some of the features observed in numerical experiments with two test problems: a planar pendulum in Cartesian coordinates and a chain molecule.

In order to make this article as self-contained as possible we give in the next two sections a brief review of the Dirac theory and the Hamilton-Dirac equations. In Section 4 we consider the extended Hamiltonian and its relationship to the Dirac theory. Section 5 specializes the theory to regular systems with imposed constraints. The following two sections contain numerical results for our test problems. Section 8 studies the constraint stability; the following section introduces the perturbed Hamiltonian state space form. Section 10 applies the obtained theoretical results to the pendulum; Section 11 studies the effect of projections. Finally, we give some conclusions.

2. THE DIRAC THEORY

Let q^i be coordinates in an N -dimensional configuration space Q . We restrict our presentation to autonomous systems, as explicit time dependencies can always be treated by considering the time as additional coordinate in an extended configuration space. The dynamics of a mechanical system described by a Lagrangian¹ $L(q, \dot{q})$ is given by the *Euler-Lagrange equations* [16]

$$(1) \quad \frac{d}{dt} \left(\frac{\partial L}{\partial \dot{q}^i} \right) - \frac{\partial L}{\partial q^i} = 0, \quad i = 1, \dots, N.$$

If the Hessian $\partial^2 L / \partial \dot{q}^i \partial \dot{q}^j$ is singular, not all equations in (1) are of second order and the system is constrained.

Introduction of the canonically conjugate momenta

$$(2) \quad p_i = \frac{\partial L}{\partial \dot{q}^i}(q, \dot{q})$$

leads to the Hamiltonian formalism. For a constrained system (2) cannot be solved for all \dot{q}^i . Instead one obtains by elimination some *primary constraints*

$$(3) \quad \phi_\alpha(q, p) = 0 \quad \alpha = 1, \dots, A \leq N.$$

The *canonical Hamiltonian* of the system is given by

$$(4) \quad H_c(q, p) = p^i \dot{q}^i - L(q, \dot{q}).$$

For an unconstrained system it is obvious that H_c can be considered as a function of (q, p) only, since \dot{q} can be eliminated using (2). Due to the special form of the right hand side of (4), this is also possible in a constrained system, but the resulting H_c is uniquely defined only *on* the constraint manifold. Thus the formalism remains unchanged, if we add an arbitrary linear combination² of the constraint

¹For simplicity we will often suppress indices, thus q, \dot{q} , etc. should be read as vectors.

²Here and in the sequel the coefficients of "linear combinations" are allowed to be arbitrary functions of the phase space variables (q, p) .

functions ϕ [18]. This leads to the *total Hamiltonian*³

$$(5) \quad H_t(q, p) = H_c + u^\alpha \phi_\alpha$$

where the multipliers u^α are a priori arbitrary functions of (q, p) .

The standard Hamiltonian formalism is based on the canonical *Poisson bracket* of two phase space functions $F(q, p), G(q, p)$

$$(6) \quad \{F, G\} = \frac{\partial F}{\partial q} \frac{\partial G}{\partial p} - \frac{\partial G}{\partial q} \frac{\partial F}{\partial p}.$$

This bracket is skew-symmetric $\{F, G\} = -\{G, F\}$ and satisfies the Jacobi identity $\{F, \{G, H\}\} + \{G, \{H, F\}\} + \{H, \{F, G\}\} = 0$. It gives the phase space the structure of a symplectic manifold. Coordinate transformations $(q, p) \mapsto (Q, P)$ that preserve this structure are called *canonical transformations*.

The time evolution of any function $F(q, p)$ is defined by

$$(7) \quad \dot{F} = \{F, H_t\}.$$

Choosing in particular $F = q$ and $F = p$, respectively, leads to the familiar form of a Hamiltonian system

$$(8) \quad \dot{q} = \frac{\partial H_t}{\partial p}, \quad \dot{p} = -\frac{\partial H_t}{\partial q}.$$

In a consistent theory the constraints $\phi_\alpha = 0$ must be preserved by the evolution of the system. This leads to the conditions

$$(9) \quad \dot{\phi}_\alpha = \{\phi_\alpha, H_t\} \approx 0.$$

The \approx signals a *weak equality*; it may hold only after taking the constraints into account. By a standard argument in differential geometry [18] this implies that the Poisson bracket in (9) must be a linear combination of the constraint functions. There are three possibilities: (i) it yields modulo the constraints an equation of the form $1 = 0$; (ii) it becomes $0 = 0$; (iii) we obtain a new equation $\psi(q, p) = 0$.

(i) implies inconsistent equations of motion; they do not possess any solution. (ii) is the desired outcome. (iii) splits into two sub-cases. If ψ depends on some of the multipliers u^α , we consider it as an equation determining one of them. Otherwise we have a *secondary constraint*. We must then check whether all secondary constraints are preserved by repeating the procedure until we either encounter case (i) or all constraints lead to case (ii). This is the *Dirac algorithm* [9, 10].

Applying the Dirac algorithm can be sometimes surprisingly subtle [18]. We consider here only a trivial example with the Lagrangian $L = \frac{1}{2}(\dot{q}^1)^2 - V(q^1, q^2)$. The momenta are $p_1 = \dot{q}^1$ and $p_2 = 0$. Thus there is one primary constraint function $\phi_1 = p_2$. The total Hamiltonian is $H_t = \frac{1}{2}p_1^2 + V(q^1, q^2) + up_2$ with a multiplier u . (9) leads to the secondary constraint function $\phi_2 = \{\phi_1, H_t\} = -V_{q^2}$. Applying again (9) yields $\{\phi_2, H_t\} = -V_{q^1 q^2} p_1 - V_{q^2 q^2} u = 0$. If we assume that $V_{q^2 q^2}$ does not vanish, the Dirac algorithm stops here, as this condition determines the multiplier u .

From the point of view of differential equations, the Dirac theory is a special case of the general problem of completing a system of differential equations. This problem is also closely related to the concept of an index of a differential algebraic equation. Essentially, the (differential) index corresponds to the number of constraint generations appearing during the Dirac algorithm [27].

³We use the Einstein convention that a summation over repeated indices is always implied.

3. HAMILTON-DIRAC EQUATIONS

Let χ_α ($\alpha = 1, \dots, K$) denote all constraint functions, primary ones and those obtained with the Dirac algorithm. They can be divided into two classes by studying the $K \times K$ matrix of their Poisson brackets

$$(10) \quad C_{\alpha\beta} = \{\chi_\alpha, \chi_\beta\} .$$

As C is skew-symmetric, its rank M is even. Let us assume for simplicity that after a simple relabeling of the χ_α the top left $M \times M$ sub-matrix of C is regular (in general we must redefine the constraint functions by taking linear combinations to achieve this). Then we call the constraint functions χ_1, \dots, χ_M *second class*.

The Poisson bracket of a *first class* constraint function ψ with any other constraint function χ (primary or higher) vanishes weakly

$$(11) \quad \forall \chi : \quad \{\psi, \chi\} \approx 0 .$$

The constraint functions $\chi_{M+1}, \dots, \chi_K$ are first class (again we may have to redefine them by taking linear combinations). Obviously this classification can be performed only after *all* constraints have been found.

First class constraints generate gauge symmetries [18]. One example is the following system which came up in a study of the quantum Hall effect [12]

$$(12) \quad L = \frac{1}{2} (q^1 - q^3 q^2)^2 + \frac{1}{2} (q^2 + q^3 q^1)^2 .$$

It describes a charged particle moving in a plane under the influence of a perpendicular constant magnetic field. There is one primary constraint function $\phi_1 = p_3$ generating one secondary constraint function $\phi_2 = q^2 p_1 - q^1 p_2$. Both are first class and essentially generate the rotational symmetry of the system.

First class constraints lead to arbitrary functions in the general solution of the equations of motion; these are under-determined [28]. In the example described by (12) q^3 remains arbitrary. In the sequel we will always assume that no first class constraints are present, as they appear very rarely in finite-dimensional systems. They can always be transformed into second class constraints by a gauge fixing.

Second class constraints signal unphysical degrees of freedom; as mentioned above their number M is always even. A trivial example is $q^1 = p_1 = 0$. If there are no first class constraints, the matrix C defined by (10) is regular and we can introduce the *Dirac bracket* [11] of two phase space functions F, G by

$$(13) \quad \{F, G\}^* = \{F, G\} - \{F, \chi_\alpha\} (C^{-1})^{\alpha\beta} \{\chi_\beta, G\} .$$

In the case of our trivial example this means that we simply omit the differentiations with respect to q^1, p_1 in (6).

The Dirac bracket has the same algebraic properties as the canonical Poisson bracket (6): it is skew-symmetric and satisfies the Jacobi identity. Hence it can be used instead of (6) to define the symplectic structure of the phase space. We show now that on the constraint manifold both brackets generate the same dynamics.

We consider the dynamics defined by

$$(14) \quad \dot{F} = \{F, H_c\}^*$$

for any function $F(q, p)$. We prove in two steps that for initial data on the constraint manifold (14) is equivalent to the original dynamics (7). It suffices to show that the right hand sides of the equations of motions (7) and (14) are weakly equal, as for such initial data the trajectories never leave the constraint manifold.

As first step we show that the evolution (14) is weakly equal to the one generated by the total Hamiltonian H_t using Dirac brackets:

$$\begin{aligned}
 \{F, H_t\}^* &= \{F, H_t\} - \{F, \chi_\alpha\} (C^{-1})^{\alpha\beta} \{\chi_\beta, H_t\} \\
 &\approx \{F, H_c\} - \{F, \chi_\alpha\} (C^{-1})^{\alpha\beta} \{\chi_\beta, H_c\} + \\
 (15) \quad &u^\gamma \left(\{F, \chi_\gamma\} - \{F, \chi_\alpha\} (C^{-1})^{\alpha\beta} \{\chi_\beta, \chi_\gamma\} \right) \\
 &= \{F, H_c\}^*.
 \end{aligned}$$

Here we used in the second line the fact that all Poisson brackets involving u^α are multiplied by constraint functions and in the last line the definition (10) of C .

As second step we note that on the constraint manifold Dirac and Poisson bracket generate the same dynamics with H_t

$$(16) \quad \{F, H_t\}^* = \{F, H_t\} - \{F, \chi_\alpha\} (C^{-1})^{\alpha\beta} \{\chi_\beta, H_t\} \approx \{F, H_t\},$$

as after completion of the Dirac algorithm $\{\chi_\beta, H_t\}$ is for all β a linear combination of constraint functions. We are thus lead to the *Hamilton-Dirac equations*

$$\begin{aligned}
 \dot{q} &= \{q, H_c\}^* = \frac{\partial H_c}{\partial p} - \frac{\partial \chi_\alpha}{\partial p} (C^{-1})^{\alpha\beta} \{\chi_\beta, H_c\}, \\
 (17) \quad \dot{p} &= \{p, H_c\}^* = -\frac{\partial H_c}{\partial q} + \frac{\partial \chi_\alpha}{\partial q} (C^{-1})^{\alpha\beta} \{\chi_\beta, H_c\}.
 \end{aligned}$$

For historical correctness one should remark that Dirac did not consider (17). He used the total Hamiltonian H_t instead of the canonical one H_c . But we proved that the corresponding equations of motion are weakly equal. Computationally the use of H_c is considerably more efficient, as it leads to simpler equations.

The Dirac bracket effectively eliminates the second class constraints, as they become *distinguished* or *Casimir functions*: the Dirac bracket of any phase space function F with a second class constraint function vanishes strongly, i. e. everywhere in phase space, as again by the definition (10) of C

$$(18) \quad \{F, \chi_\gamma\}^* = \{F, \chi_\gamma\} - \{F, \chi_\alpha\} (C^{-1})^{\alpha\beta} \{\chi_\beta, \chi_\gamma\} = 0.$$

4. THE EXTENDED HAMILTONIAN

The distinction into first and second class constraints is an intrinsic one, i. e. it has a geometric meaning. In contrast, the distinction into primary and secondary (or higher) constraints is to some extent artificial and depends on the precise form of the Lagrangian L . There might exist an equivalent Lagrangian, i. e. one describing the same system, yielding different primary constraints.

Furthermore, if one looks at the argument for introducing the total Hamiltonian, one sees that one could also apply it to secondary constraints. These considerations lead to the *extended Hamiltonian* H_e which is the canonical Hamiltonian H_c plus a linear combination of *all* constraint functions and not just the primary ones as in the definition of H_t .

This approach was studied by Leimkuhler and Reich [20] while searching for a way to integrate symplectically a constrained Hamiltonian system. By calling H_e extended Hamiltonian we slightly abuse Dirac's terminology. He added only the first class class constraint functions based on symmetry and not on stability considerations.

Assuming that all constraint functions χ are second class we make the ansatz

$$(19) \quad H_e = H_c + v^\alpha \chi_\alpha .$$

Recall that the v should not be considered as new variables but as so far unknown functions of (q, p) ! Demanding $\{\chi_\alpha, H_e\} \approx 0$ yields the condition

$$(20) \quad \{\chi_\alpha, H_e\} = \{\chi_\alpha, H_c\} + \{\chi_\alpha, v^\beta\} \chi_\beta + \{\chi_\alpha, \chi_\beta\} v^\beta \approx 0 ,$$

If we discard the Poisson brackets with v , since they are multiplied by constraint functions, (20) becomes a system of linear equations with the particular solution

$$(21) \quad v^\alpha = -(C^{-1})^{\alpha\beta} \{\chi_\beta, H_c\}$$

with C given by (10). Further solutions of the weak equation (20) are obtained by adding an arbitrary linear combination of constraint functions to each of the v^α .

This suggests the following equations of motion

$$(22) \quad \dot{q} = \{q, H_e\} , \quad \dot{p} = \{p, H_e\} .$$

We will see below that they yield the correct dynamics, as (22) is weakly equal to the equations derived with the total Hamiltonian H_t .

The extended Hamiltonian leads to considerably more involved equations of motion than the Hamilton-Dirac approach. The multipliers and thus H_e depend on the matrix C^{-1} also appearing in the Dirac bracket (13). The equations of motion contain terms arising from the Poisson brackets of the dynamical variables with the entries of C^{-1} and these terms are typically rather complicated.

Leimkuhler and Reich considered a simplification which they called the “weakly Hamiltonian Dirac formulation”. It arises by discarding the terms containing the Poisson brackets with the multipliers. This is allowed, since they vanish weakly. Using the solution (21) for the multipliers we obtain as equations of motion

$$(23) \quad \begin{aligned} \dot{q} &= \{q, H_e\} \approx \{q, H_c\} - \{q, \chi_\alpha\} (C^{-1})^{\alpha\beta} \{\chi_\beta, H_c\} , \\ \dot{p} &= \{p, H_e\} \approx \{p, H_c\} - \{p, \chi_\alpha\} (C^{-1})^{\alpha\beta} \{\chi_\beta, H_c\} . \end{aligned}$$

Thus we recover the Hamilton-Dirac equations (17)! Leimkuhler and Reich claimed that they were not Hamiltonian. We can now correct this statement. Although (17) is not Hamiltonian with respect to the canonical Poisson bracket, it is with respect to the Dirac bracket.

This derivation of the extended Hamiltonian H_e is a special case of a more general construction [32]. With any phase space function A we can associate a function $A^* \approx A$ such that $\{A^*, \chi\} \approx 0$ for all constraint functions χ

$$(24) \quad A^* = A - \chi_\alpha (C^{-1})^{\alpha\beta} \{\chi_\beta, A\} .$$

Using (21) for the multipliers we find $H_e = H_c^*$. The Dirac bracket of two functions A, B is weakly equal to the Poisson bracket of their associated quantities

$$(25) \quad \{A, B\}^* \approx \{A^*, B^*\} .$$

5. REGULAR SYSTEMS WITH IMPOSED CONSTRAINTS

For applications the most important case of a constrained system is described by a regular Lagrangian L_0 and subject to m externally imposed holonomic constraints $\phi_\alpha(q) = 0$. In principle, this situation *cannot* be treated within the Dirac formalism, as it covers only singular Lagrangians. Therefore one introduces Lagrange multipliers λ^α and considers the Lagrangian $L = L_0 + \lambda^\alpha \phi_\alpha$. In contrast to

the multipliers u in the Dirac theory, the λ must be considered as additional dynamical variables and not as undetermined functions. Then L is obviously singular, as it does not depend on the “velocities” λ .

To pass to the Hamiltonian formalism we must introduce canonically conjugate momenta π_α for the λ^α . The primary constraints are simply given by $\pi = 0$. If we denote by H_0 the Hamiltonian for the regular system, the canonical Hamiltonian of the constrained system is $H_c = H_0 - \lambda^\alpha \phi_\alpha$; the total one is $H_t = H_c + u^\alpha \pi_\alpha$. The Dirac algorithm yields the secondary constraints $\phi_\alpha = 0$ and the tertiary constraints $\psi_\alpha = \{\phi_\alpha, H_0\} = 0$. The next step gives equations for λ

$$(26) \quad \{\psi_\alpha, H_0\} - \lambda^\beta \{\psi_\alpha, \phi_\beta\} = 0.$$

The fifth and last step yields $u = 0$.

This rather long derivation can be shortened by *not* introducing the total Hamiltonian H_t and the momenta π . Starting with H_c and imposing $\phi = 0$ as primary constraints leads to equivalent results, as in the end $\pi = u = 0$. The standard approach is to take the Hamiltonian equations of motion for H_c and augment them by the constraints to get the following differential algebraic equation

$$(27) \quad \dot{q} = \frac{\partial H_0}{\partial p}, \quad \dot{p} = -\frac{\partial H_0}{\partial q} + \lambda^\alpha \frac{\partial \phi_\alpha}{\partial q}, \quad \phi_\alpha = 0.$$

By differentiating twice the last equation in (27) one can derive exactly the same equation (26) for λ as in the Dirac theory. With $Q_{\alpha\beta} = \{\phi_\alpha, \psi_\beta\}$ it has the solution

$$(28) \quad \lambda^\alpha \approx (Q^{-1})^{\alpha\beta} \{\psi_\alpha, H_0\}.$$

The main problem in using Dirac brackets is the inversion of the matrix C of the Poisson brackets of the constraint functions. For a larger number M of constraints one can no longer do this symbolically. Thus one must numerically invert an $M \times M$ matrix at each evaluation of the equations of motion. In our special case $M = 2m$ and C can be partitioned into four $m \times m$ sub-matrices

$$(29) \quad C = \begin{pmatrix} 0 & Q \\ -Q^t & S \end{pmatrix}$$

where Q is as above and $S_{\alpha\beta} = \{\psi_\alpha, \psi_\beta\}$. The inversion of such a matrix can be reduced to the inversion of one $m \times m$ matrix plus two matrix multiplications, as

$$(30) \quad C^{-1} = \begin{pmatrix} Q^{-t} S Q^{-1} & -Q^{-t} \\ Q^{-1} & 0 \end{pmatrix}.$$

The Hamilton-Dirac equations take now the following form

$$(31) \quad \begin{aligned} \dot{q} &= \frac{\partial H_0}{\partial p} - (Q^{-1})^{\alpha\beta} \frac{\partial \psi_\alpha}{\partial p} \psi_\beta, \\ \dot{p} &= -\frac{\partial H_0}{\partial q} - (Q^{-1})^{\alpha\beta} \frac{\partial \phi_\alpha}{\partial q} \{\psi_\beta, H_0\} \\ &\quad + \left[(Q^{-t} S Q^{-1})^{\alpha\beta} \frac{\partial \phi_\alpha}{\partial q} + (Q^{-1})^{\alpha\beta} \frac{\partial \psi_\alpha}{\partial q} \right] \psi_\beta. \end{aligned}$$

Taking (28) into account we see that they differ from (27) only by some terms multiplied by ψ . Thus both formulations are weakly equal. Note that the position constraint functions ϕ do not appear!

This implies that we cannot apply the results of Ascher *et al.* [4] on the stabilization of general differential algebraic equations. They also transform the constraint

functions into invariants and add them multiplied by some regular matrix to an underlying differential equation. Under some additional assumptions they could show that the constraint manifold is asymptotically stable for the obtained flow.

The Hamilton-Dirac equations can be understood within this general scheme, but the results do not hold, as the corresponding matrix is singular. Thus we find weaker stability results. But we still have a Hamiltonian system, whereas their approach generally destroys this property.

For the extended Hamiltonian we make the following ansatz (note the different sign for λ compared with the last section)

$$(32) \quad H_e = H_0 - \lambda^\alpha \phi_\alpha + \mu^\alpha \psi_\alpha.$$

For λ we recover the result (28); for μ we obtain

$$(33) \quad \mu^\alpha = (Q^{-1})^{\alpha\beta} \psi_\beta.$$

Thus μ vanishes weakly und could be taken as zero.

The multipliers λ depend on derivatives of the momentum constraint functions ψ . Since they occur in the extended Hamiltonian H_e , we need three differentiations of the original constraint functions ϕ to set up the equations of motion opposed to the Hamilton-Dirac equations where two differentiations suffice.

6. EXAMPLE I: THE PENDULUM

A classical example of a constrained system is the planar pendulum in Cartesian coordinates. For simplicity, all constants like length, mass, etc. are set to 1. The Lagrangian of the underlying regular system is $L_0 = \frac{1}{2}(\dot{x}^2 + \dot{y}^2) - y$. We add the constraint function $\phi = \frac{1}{2}(x^2 + y^2 - 1)$ with a multiplier λ to get the Lagrangian for the pendulum $L = L_0 + \frac{1}{2}\lambda(x^2 + y^2 - 1)$. The canonically conjugate momenta are just the velocities: $p_x = \dot{x}$, $p_y = \dot{y}$. Checking whether the evolution generated by the Hamiltonian $H_t = \frac{1}{2}(p_x^2 + p_y^2) + y - \frac{1}{2}\lambda(x^2 + y^2 - 1)$ preserves the primary constraint $\phi = 0$ yields a secondary constraint $\psi = \{\phi, H_t\} = xp_x + yp_y = 0$. Then the Dirac algorithm stops, as the next step only determines λ . Since $\{\phi, \psi\} = x^2 + y^2$ the Dirac bracket takes the form

$$(34) \quad \{F, G\}^* = \{F, G\} + \frac{1}{x^2 + y^2} \left(\{F, \phi\} \{\psi, G\} - \{F, \psi\} \{\phi, G\} \right).$$

By taking Dirac brackets with the Hamiltonian $H_0 = (p_x^2 + p_y^2)/2 + y$ of the underlying regular system we finally arrive at the Hamilton-Dirac equations,

$$(35) \quad \dot{x} = p_x + \mu x, \quad \dot{y} = p_y + \mu y, \quad \dot{p}_x = \lambda x - \mu p_x, \quad \dot{p}_y = \lambda y - \mu p_y - 1,$$

where λ, μ are given by

$$(36) \quad \lambda = -\frac{p_x^2 + p_y^2 - y}{x^2 + y^2}, \quad \mu = -\frac{xp_x + yp_y}{x^2 + y^2}.$$

We compare this formulation with the one based on the extended Hamiltonian $H_e = H_0 - \lambda\phi + \mu\psi$ with the multipliers λ, μ again given by (36). This corresponds

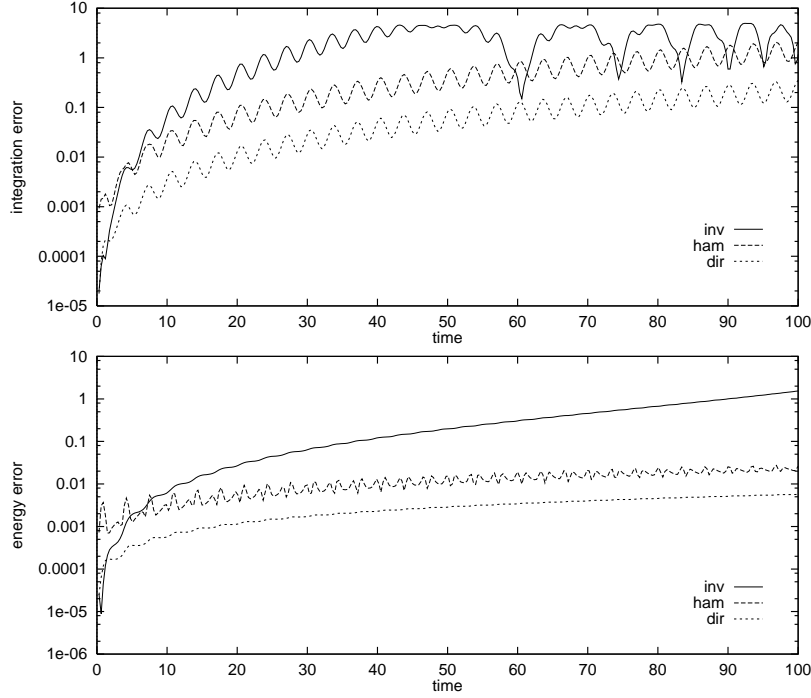


FIGURE 1. Integration and energy error (pendulum)

to the choice (21) for the solution of (20). The equations of motion are

$$\begin{aligned}
 \dot{x} &= \left(2 - \frac{1}{x^2 + y^2}\right) p_x + 2\mu x, & \dot{y} &= \left(2 - \frac{1}{x^2 + y^2}\right) p_y + 2\mu y, \\
 \dot{p}_x &= \lambda \frac{x}{x^2 + y^2} - 2\mu p_x - 2\mu^2 x, \\
 \dot{p}_y &= \lambda \frac{y}{x^2 + y^2} - 2\mu p_y - 2\mu^2 y - \frac{1}{2} \left(1 + \frac{1}{x^2 + y^2}\right).
 \end{aligned}
 \tag{37}$$

They differ from (35) only by linear combinations of constraint functions. As expected, they are more complicated and thus more expensive to evaluate.

In order to show the necessity of stabilizing the constraint manifold we compare these two formulations with the following naive approach: construct an underlying ordinary differential equation by differentiating the constraints, choose initial data satisfying all constraints and ignore them thereafter. This yields the equations of motion (with λ again given by (36))

$$\dot{x} = p_x, \quad \dot{y} = p_y, \quad \dot{p}_x = \lambda x, \quad \dot{p}_y = \lambda y - 1.
 \tag{38}$$

We integrated numerically all three formulations for the following initial data: $x^0 = 1$, $y^0 = 0$, $p_x^0 = 0$, $p_y^0 = -2$. For these values the pendulum rotates clockwise with a period of $T \approx 3.31$. We integrated over the interval $t \in [0, 100]$, i. e. roughly over 30 periods, with a constant step size of $h = 0.1 \approx T/33$. Fig. 1 contains logarithmic plots of the integration and the energy error, Fig. 2 of the position and velocity constraint residuals. **inv**, **ham** and **dir** label the curves for the naive equations of motion (38), for the equations (37) derived with the extended Hamiltonian

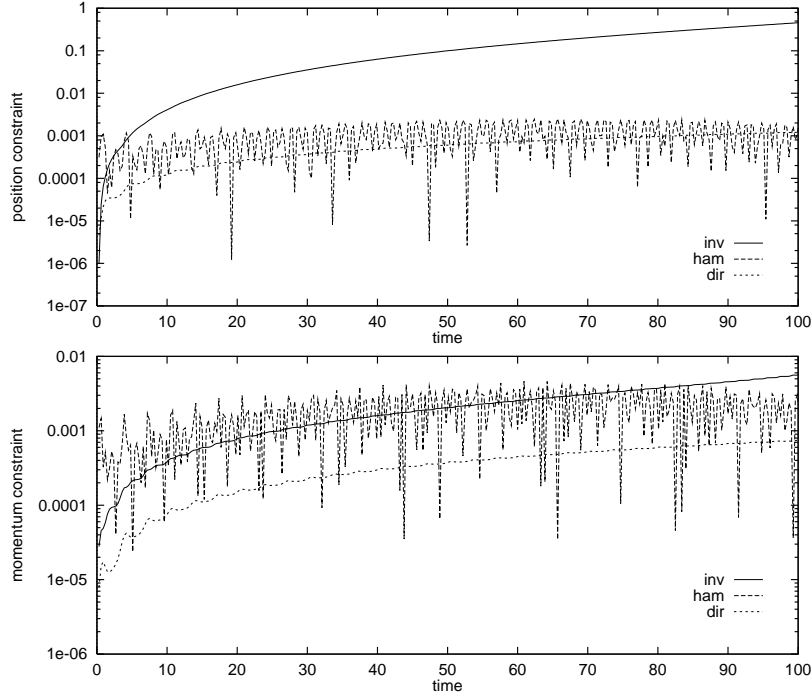


FIGURE 2. Position and momentum constraint residual (pendulum)

and for the Hamilton-Dirac equations (35), respectively. The integration error was estimated by comparing with the solution of the state space form $\ddot{\varphi} = -\sin \varphi$ computed with $h/10$.

Since the amplitude of our pendulum is 1 and its maximal momentum about 2.45, the computed values can surely be considered as useless, if the integration error exceeds 1. Thus the Hamilton-Dirac equations are the only formulation where the numerical integration does not clearly break down before the end of the considered interval. With the extended Hamiltonian one obtains reasonable results until approximately $t = 70$; with the naive formulation perhaps until $t = 30$.

The stabilizing effect of the extended Hamiltonian and of the Dirac brackets, respectively, shows not only in the lower absolute values of the errors but also in their growth. Both formulations show a quadratic growth of the integration error and a linear growth of the energy error. Taking only the time into account where the naive formulation yields reasonable results, its integration error grows cubically and its energy error quadratically. For the Hamilton-Dirac equations the constraint residuals grow linearly, for the extended Hamiltonian even less. In the naive formulation the position constraint residual shows a quadratic growth, whereas the momentum constraint residual behaves also linearly.

Another aspect is how much of the periodicity of the solution is maintained during the numerical integration. Table 1 contains the numerical values of y after several revolutions. The correct value would be zero for our initial data. Phase portraits of the numerical solutions (not shown here) also clearly demonstrate that the

	$y(2T)$	$y(4T)$	$y(10T)$	$y(20T)$	$y(30T)$
inv	$9.66 \cdot 10^{-3}$	$7.28 \cdot 10^{-2}$	$9.22 \cdot 10^{-1}$	$2.16 \cdot 10^{-1}$	$3.05 \cdot 10^{-1}$
ham	$5.75 \cdot 10^{-3}$	$1.77 \cdot 10^{-2}$	$8.98 \cdot 10^{-2}$	$3.17 \cdot 10^{-1}$	$6.21 \cdot 10^{-1}$
dir	$8.28 \cdot 10^{-4}$	$2.63 \cdot 10^{-3}$	$1.39 \cdot 10^{-2}$	$5.18 \cdot 10^{-2}$	$1.13 \cdot 10^{-1}$

TABLE 1. Phase error (pendulum)

naive formulation leads only for rather short times to an acceptable approximation of the true solution.

In a comparison one must also take the computational costs into account. Using the Hamilton-Dirac equations requires only about 5% more computing time than the naive formulation, whereas the extended Hamiltonian needs almost 65% more time. The difference in computational efficiency becomes even larger with a variable step size. Using a fifth order Runge-Kutta-Fehlberg method the integration of the equations of motion derived with the extended Hamiltonian needs between 50% and 100% more evaluations of the equations for the same prescribed precision than the Dirac bracket approach.

7. EXAMPLE II: A CHAIN MOLECULE

As a larger example we consider a problem in molecular dynamics already used by Leimkuhler and Skeel [21] in the context of constrained dynamics. It consists of a planar chain molecule with $N = 7$ atoms. The bonds between them are assumed to have a fixed length. This condition yields the constraints. The interaction of the atoms is described by a Lennard-Jones potential

$$(39) \quad V = 0.1 \sum_{j>i} (r_{ij}^{-12} - 2r_{ij}^{-6})$$

where r_{ij} denotes the distance between atom i and atom j .

One global energy minima of the molecule is the hexagonal structure shown in the left part of Fig. 3. We will take this as initial configuration in our computations. At the ends of the chain we start with initial velocities of equal amplitude ($v_0 = 0.25$) but opposite direction; the remaining atoms are initially at rest. The emerging dynamics can be split into a rigid body rotation of the whole chain and small vibrations of each atom around its equilibrium position. The right part of Fig. 3 shows the motion of an end atom of the chain.

Integration methods for differential algebraic systems are often based on backward differentiation formulae. As Leimkuhler and Skeel [21] reported, this approach leads to physically unacceptable solutions. Such methods were originally developed for stiff systems. After a short time they completely eliminate the vibrational degrees of freedom of the system and yield a pure rigid body rotation. This implies a significant violation of energy conservation.

We choose this model in order to demonstrate that the Dirac bracket approach can be reasonably applied even for larger systems. Actually in this example it is still easily possible to perform all necessary calculations by hand based on our results in Section 5. We did not try to do this for the method of the extended Hamiltonian, as it would lead to very complex equations of motion.

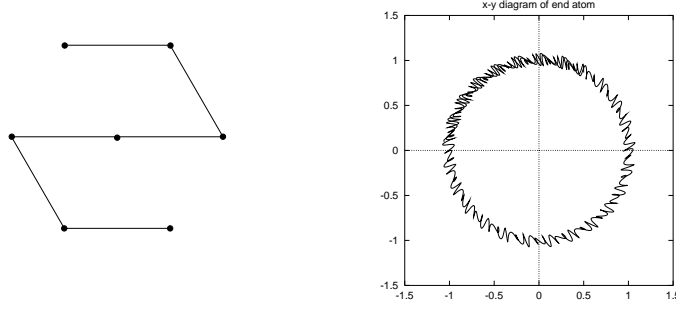


FIGURE 3. Global energy minimum and motion of end atom

If we denote the coordinates of atom i by (x^i, y^i) and its momenta by p_x^i, p_y^i , the underlying regular Hamiltonian is

$$(40) \quad H_0 = \frac{1}{2} \sum_{i=1}^N \left[(p_x^i)^2 + (p_y^i)^2 \right] + V(x, y)$$

with V given by (39). The constraints are

$$(41) \quad \begin{aligned} \phi_\alpha &= \frac{1}{2} [(\Delta x^\alpha)^2 + (\Delta y^\alpha)^2 - L^2] = 0, & \alpha = 1, \dots, 6, \\ \psi_\alpha &= \Delta x^\alpha \Delta p_x^\alpha + \Delta y^\alpha \Delta p_y^\alpha = 0, \end{aligned}$$

where L stands for the length of the bonds and where we have introduced the short hand $\Delta x^\alpha = x^\alpha - x^{\alpha+1}$ and so on.

Computing the entries of the matrices Q, S defined in Section 5 we obtain for Q

$$(42) \quad \begin{aligned} \{\phi_\alpha, \psi_\beta\} &= 2\delta_{\alpha\beta} [(\Delta x^\alpha)^2 + (\Delta y^\alpha)^2] - \\ &\quad \delta_{\alpha+1, \beta} [\Delta x^\alpha \Delta x^\beta + \Delta y^\alpha \Delta y^\beta] - \\ &\quad \delta_{\alpha, \beta+1} [\Delta x^\beta \Delta x^\alpha + \Delta y^\beta \Delta y^\alpha] \end{aligned}$$

and for S , respectively,

$$(43) \quad \begin{aligned} \{\psi_\alpha, \psi_\beta\} &= \delta_{\alpha+1, \beta} [\Delta x^\alpha \Delta p_x^\beta - \Delta x^\beta \Delta p_x^\alpha + \Delta y^\alpha \Delta p_y^\beta - \Delta y^\beta \Delta p_y^\alpha] - \\ &\quad \delta_{\alpha, \beta+1} [\Delta x^\beta \Delta p_x^\alpha - \Delta x^\alpha \Delta p_x^\beta + \Delta y^\beta \Delta p_y^\alpha - \Delta y^\alpha \Delta p_y^\beta]. \end{aligned}$$

Both matrices are tridiagonal, as we have a chain structure or “nearest neighbors constraints:” ϕ_α, ψ_α involve only data of the atoms α and $\alpha + 1$. The inversion of such matrices has a linear complexity and can thus be done very fast.

The Poisson brackets of the coordinates with the constraint functions are

$$(44) \quad \begin{aligned} \{x^i, \phi_\alpha\} &= 0, \\ \{p_x^i, \phi_\alpha\} &= -\{x^i, \psi_\alpha\} = (\delta_{\alpha+1}^i - \delta_\alpha^i) \Delta x^\alpha, \\ \{p_x^i, \psi_\alpha\} &= (\delta_{\alpha+1}^i - \delta_\alpha^i) \Delta p_x^\alpha \end{aligned}$$

and corresponding expressions for y, p_y . Finally, we calculate

$$(45) \quad \begin{aligned} \{\psi_\alpha, H_0\} &= (\Delta p_x^\alpha)^2 + (\Delta p_y^\alpha)^2 - \\ &\quad \Delta x^\alpha \left(\frac{\partial V}{\partial x^\alpha} - \frac{\partial V}{\partial x^{\alpha+1}} \right) - \Delta y^\alpha \left(\frac{\partial V}{\partial y^\alpha} - \frac{\partial V}{\partial y^{\alpha+1}} \right). \end{aligned}$$

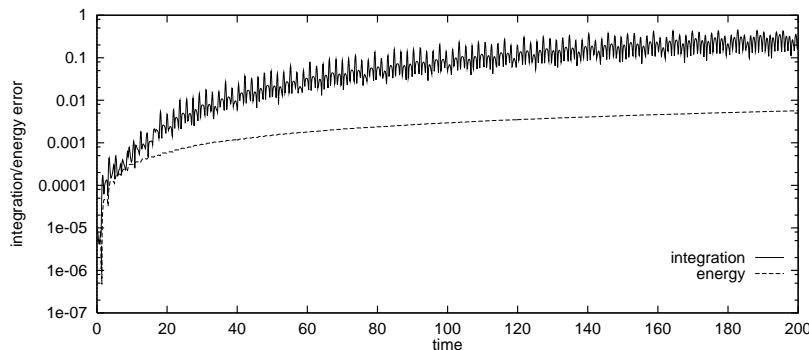


FIGURE 4. Integration and energy error (chain molecule)

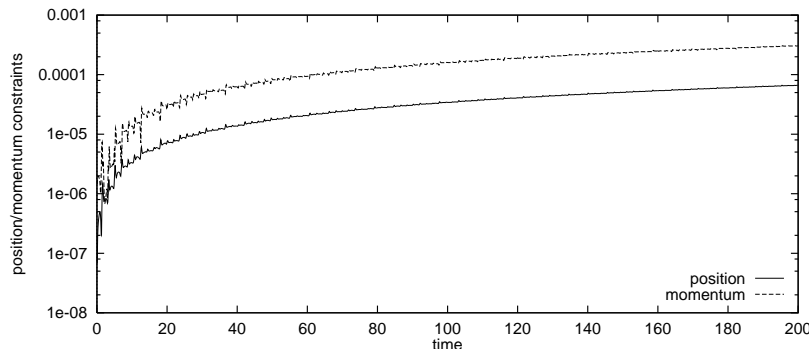


FIGURE 5. Position and momentum constraint residuals (chain molecule)

(42–45) contain all expressions needed to define the Dirac bracket. Setting up the equations of motion (31) is now straightforward. The evaluation of the potential and the two matrix multiplications have a complexity quadratic in the number N of atoms. All other operations are linear in N . Thus Dirac brackets could be applied without problems even for much larger molecules.

We integrated the system with the initial conditions described above with the fourth-order Runge-Kutta method for the interval $t \in [0, 200]$. As one can see from the right part of Fig. 3 this corresponds roughly to $5/4$ periods of the rigid body rotation of the molecule. Figs. 4 and 5 show the result for the constant step size $h = 0.1$. As for the Hamilton-Dirac formulation of the pendulum, the integration error grows quadratically, all others errors about linearly.

Comparing with Leimkuhler and Skeel [21], we find that at least regarding energy conservation their approach using the RATTLE algorithm [3] leads to better results. Their energy error remains more or less constant over the full integration interval $t \in [0, 200]$. The explanation is simple: RATTLE is a *symplectic integrator* [25].

It is well-known that such methods often perform superior in long time integrations, especially with respect to energy conservation. Since almost all known symplectic integrators preserve only the canonical Poisson bracket, it may appear that they are not applicable in the case of a modified bracket structure like the Dirac bracket used in the Hamilton-Dirac equations.

We hope to discuss this problem in more detail in the future, but we want to comment briefly on some preliminary experiments with a *canonical* symplectic integrator: the implicit midpoint rule. The arising nonlinear equations were solved with a simple functional iteration to a tolerance of 10^{-5} .

Although the implicit midpoint rule is only second order opposed to the fourth-order scheme used so far, it conserved the energy for the same step size better by almost an order of magnitude. The error growth is less than linear; the constraints residuals improve by more than an order of magnitude. If the step size is halved, the energy error becomes smaller by more than an order of magnitude and remains almost constant about 10^{-4} over the full integration interval.

A partial explanation might be given as follows. On the constraint manifold the Dirac bracket represents the symplectic structure induced by the canonical Poisson bracket [18, 30] (see also Section 9). As long as the constraint residuals remain small, a canonical symplectic integrator thus defines in good approximation a symplectic mapping for the Dirac bracket, too. But for other approaches [19, 24] to the symplectic integration of constrained systems the situation does not differ much, as these methods require the solution of nonlinear equations and are truly symplectic only, if the equations are solved exactly. In a numerical computation they are also only approximations of symplectic mappings.

The implicit midpoint rule preserves quadratic first integrals, if the arising nonlinear equations are solved exactly [7]. In our example the constraints and the energy are defined by quadratic functions. The constraints are first integrals for the Hamilton-Dirac equations; this is an important difference to the extended Hamiltonian where they are only weak invariants. Therefore it is not surprising that we find small errors.

We may expect that the higher the precision with which the nonlinear equations are solved, the more the implicit midpoint rule behaves like a true symplectic integrator for the Dirac bracket. First numerical tests seem to confirm this conjecture. In the case of the pendulum one observes for example much smaller phase errors compared with Table 1.

Finally, the chain molecule possesses at least two more integrals of motion besides the energy: total linear and total angular momentum. Independent of the integration method, both are preserved with rather high accuracy: the error in the latter one lies between 10^{-5} and 10^{-6} , for the former one it is about 10^{-15} . But that is again not surprising, as any Runge-Kutta method preserves linear conservation laws and the angular momentum is also a quadratic first integral.

8. CONSTRAINT STABILITY

The fundamental problem in the numerical integration of differential algebraic equations is the drift off the constraint manifold. We split our study of the stability of constrained Hamiltonian systems against this drift into two parts: in this section we consider solely the constraints; in the next section we develop a perturbed Hamiltonian state space form.

For a Hamiltonian system with $M = 2m$ second class constraints there exists, at least locally, a canonical transformation $(q, p) \mapsto (Q, P)$ such that in the new coordinates the constraints take the simple form $Q^\alpha = P_\alpha = 0$ for $\alpha = 1, \dots, m$ [18]. Let us assume that after this change of coordinates the equations of motion decouple into one system for (Q^α, P_α) and one for the remaining coordinates.

The latter one represents the dynamics of the true degrees of freedom. The former one has the origin as a fixed point, since the time derivative of any constraint function is a linear combination of constraint functions (see below). The stability of this fixed point gives an indication of the stability of the constraint manifold. If it is unstable, small deviations are amplified by the dynamics leading to the often observed explosive growth of the constraint residuals.

In general, the equations of motion do not decouple. Nevertheless it is still useful to split into two subsystems as above. If some of the true dynamical variables (Q^k, P_k) with $k > m$ occur in the subsystem for the constraint residuals, we may consider them in the stability analysis as time dependent parameters. If (Q^α, P_α) appear in the other subsystem, any error in the constraints yields an additional perturbation of the true dynamics.

Thus we can split the stability analysis into two parts: (A) study the evolution of the redundant coordinates, (B) study the evolution of the true degrees of freedom. The explicit construction of the canonical transformation $(q, p) \mapsto (Q, P)$ is usually only possible for simple systems. Part (A) can nevertheless be done at least partially by analyzing the evolution of the constraint functions.

Independent of how we set up the equations of motion, the time derivative of any constraint function χ_α must vanish weakly. Otherwise we would have an inconsistent theory. By the same differential geometric argument as used in Section 2 for the analysis of (9) we can write

$$(46) \quad \dot{\chi}_\alpha = A_\alpha^\beta \chi_\beta$$

with some coefficients $A_\alpha^\beta(q, p)$. Considered as a linear system of ordinary differential equations for χ (with in general time varying coefficients), (46) has obviously a fixed point at the origin $\chi = 0$. Its stability depends on the matrix A .

For the Hamilton-Dirac equations (17) the stability analysis of (46) is easy. Since according to (18) the constraint functions χ_α are distinguished functions, we have

$$(47) \quad \dot{\chi}_\alpha = \{\chi_\alpha, H_c\}^* = 0.$$

Thus the constraint functions are invariants or first integrals of the flow generated by (17) and the origin $\chi_\alpha = 0$ is stable though not asymptotically stable.

This has the following geometric implications. The constraint functions χ divide the phase space into disjoint subspaces \mathcal{M}_ϵ defined by $\chi_\alpha(q, p) = \epsilon_\alpha$ with constants ϵ . Exact solutions of the Hamilton-Dirac equations (17) always lie completely on the subspace \mathcal{M}_ϵ determined by the initial data. The Hamilton-Dirac equations do not “see” the values ϵ ; especially $\epsilon = 0$ is not distinguished.⁴ Numerical errors are neither damped nor amplified by the dynamics. They lead to different values $\bar{\epsilon}$ and without further numerical errors the trajectory would stay on the subspace $\mathcal{M}_{\bar{\epsilon}}$.

Under some additional assumptions we can even get a quantitative estimate for the drift in the constraints. Let us model the numerical errors by introducing a perturbation into the equations of motion: instead of (17) we consider

$$(48) \quad \dot{q} = \{q, H_c\}^* + \delta_q(t), \quad \dot{p} = \{p, H_c\}^* + \delta_p(t)$$

⁴This is also evident from the fact that the Dirac bracket depends only on derivatives of the constraint functions and not on the functions themselves.

for some functions δ_q, δ_p . Then we get instead of (47) the equations

$$(49) \quad \dot{\chi}_\alpha = \frac{\partial \chi_\alpha}{\partial q} \delta_q + \frac{\partial \chi_\alpha}{\partial p} \delta_p.$$

Assuming that in the considered time interval the vectors δ_q, δ_p and the matrices $\partial \chi / \partial q, \partial \chi / \partial p$ are all bounded (in a suitable norm) by some constant, we find by a simple integration of (49) that the constraint residuals grow at most linearly in time. With a similar argument one can show that the energy error grows linearly, if one assumes that $\partial H / \partial q$ and $\partial H / \partial p$ are bounded by a constant, too.

Alishenas [1] performed a similar analysis for the Euler-Lagrange equations of regular systems with imposed constraints. There one finds that while the error in the velocity constraints (which correspond to our momentum constraints $\psi = 0$) also grows linearly, the position constraint residuals show a quadratic growth. Thus the Hamilton-Dirac equations preserve the constraints better.

For the approach based on the extended Hamiltonian we cannot derive such general results. The precise form of the matrix A depends here crucially on the chosen solution of the linear system (20) for the multipliers v . Using (21) we get the following complicated expression for A

$$(50) \quad A_\alpha^\beta = -\{\chi_\alpha, (C^{-1})^{\beta\gamma} \{\chi_\gamma, H_c\}\}$$

where again $C_{\alpha\beta} = \{\chi_\alpha, \chi_\beta\}$.

Leimkuhler and Reich [20] showed for the special case of the pendulum that with one choice the origin is a center, whereas with another choice it is a saddle point. In the notation of Section 5 the fixed point is a center, if we use (28,33) for determining λ, μ (see also Section 10). If we try to obtain simpler equations of motion by exploiting the fact that μ vanishes weakly and set it to zero, the fixed point becomes an unstable saddle point. In principle, one could use this stability analysis as a guideline for choosing the precise form of the multipliers. But this seems hardly feasible in practice.

9. PERTURBED HAMILTONIAN STATE SPACE FORM

If we restrict to regular systems with m imposed constraints $\phi_\alpha(q) = 0$ where the Hamiltonian is separable and of the form $H_0(q, p) = \frac{1}{2}p^t p + V(q)$, we can to some extent also perform part (B) of the stability analysis using again a perturbation approach. We assume that the constraint functions are irreducible, i. e. their Jacobian has rank m . As explained in Section 5, the Dirac algorithm yields the secondary constraints $\psi_\alpha = (\partial \phi_\alpha / \partial q)p = 0$ and no further ones.

For such systems we construct a symplectic mapping from the manifolds $\mathcal{M}_{\zeta, \rho}$ defined by $\phi_\alpha = \zeta^\alpha, \psi_\alpha = \rho_\alpha$ for some fixed but arbitrary values $\zeta^\alpha, \rho_\alpha$ into a reduced $2(N - m)$ -dimensional phase space \mathcal{P} . Let $\xi^a, \pi_a, a = 1, \dots, N - m$ be canonical coordinates for \mathcal{P} , i. e. in \mathcal{P} the canonical Poisson bracket of two functions $A(\xi, \pi), B(\xi, \pi)$ is given by

$$(51) \quad \{A, B\} = \frac{\partial A}{\partial \xi} \frac{\partial B}{\partial \pi} - \frac{\partial A}{\partial \pi} \frac{\partial B}{\partial \xi}.$$

By the implicit function theorem there exist N functions $f^i(\xi, \zeta)$ such that

$$(52) \quad \phi_\beta(f(\xi, \zeta)) = \zeta^\beta.$$

The equations

$$(53) \quad q^i = f^i(\xi, \zeta), \quad \frac{\partial f^i}{\partial \xi^a} p_i = \pi_a, \quad \frac{\partial \phi_\alpha}{\partial q^i} p_i = \rho_\alpha$$

define implicitly a mapping $,_{\zeta, \rho} : (q, p) \in \mathcal{M}_{\zeta, \rho} \mapsto (\xi, \pi) \in \mathcal{P}$. It is symplectic, as it can be derived from the generating function $S(\xi, p) = f^i(\xi, \zeta) p_i$ [16]. Indeed we find that $q^i = \partial S / \partial p_i$, $\pi_a = \partial S / \partial \xi^a$.

Let $F(q, p)$ be a phase space function. We can associate with its restriction to $\mathcal{M}_{\zeta, \rho}$ a function $\tilde{F}(\xi, \pi)$ defined on \mathcal{P} by $F = \tilde{F} \circ ,_{\zeta, \rho}$. Because $,_{\zeta, \rho}$ is a symplectic mapping, we find

$$(54) \quad \widetilde{\{F, G\}} = \{\tilde{F}, \tilde{G}\}$$

where the Poisson bracket on the left hand side is defined by (6) and the one on the right hand side by (51). Thus it does not matter whether we first restrict to $\mathcal{M}_{\zeta, \rho}$ and then compute the Poisson bracket or the other way round.

In the full phase space the Dirac bracket (13) differs from the canonical Poisson bracket (6). But on each submanifold $\mathcal{M}_{\zeta, \rho}$ it represents the bracket induced by the canonical Poisson bracket [18, 30]. Thus we may substitute the Poisson bracket on the left hand side of (54) by the Dirac bracket and obtain

$$(55) \quad \widetilde{\{F, G\}}^* = \{\tilde{F}, \tilde{G}\}.$$

Because of (55) we get a perturbed state space form essentially by computing the transformed Hamiltonian \tilde{H}_0 . With the short hand f_ξ for the Jacobian of the f with respect to ξ and ϕ_q for the Jacobian of the constraint functions one finds (using $\phi_q f_\xi = 0$)

$$(56) \quad \tilde{H}_0(\xi, \pi) = \frac{1}{2} \pi^t \left(f_\xi^t f_\xi \right)^{-1} \pi + \frac{1}{2} \rho^t \left(\phi_q \phi_q^t \right)^{-1} \rho + V \circ f$$

and the perturbed Hamiltonian state space form is

$$(57) \quad \dot{\xi} = \{\xi, \tilde{H}_0\}, \quad \dot{\pi} = \{\pi, \tilde{H}_0\}$$

with the Poisson bracket given by (51). An unperturbed Hamiltonian state space form is obtained by setting $\zeta = \rho = 0$. It is identical with the one introduced by Leimkuhler and Reich [20].

We can refine the perturbation analysis by considering ζ, ρ as time-dependent. This does not change the symplectic mapping $,_{\zeta, \rho}$, but we must subtract from \tilde{H}_0 as given by (56) the time derivative of the generating function [16]

$$(58) \quad \frac{\partial S}{\partial t} = \dot{\zeta}^t f_\zeta^t \left(\begin{matrix} f_\xi^t \\ \phi_q \end{matrix} \right)^{-1} \left(\begin{matrix} \pi \\ \rho \end{matrix} \right).$$

Due to the relation (55) between the canonical Poisson bracket in \mathcal{P} and the Dirac bracket, (57) may be considered as the result of a simple canonical transformation applied to the Hamilton-Dirac equations, although both systems live in phase spaces of different dimensions. We can thus get information about the stability of the Hamilton-Dirac equations by analyzing how the parameters ζ, ρ enter (57).

The function f in (56) depends on ζ ; this yields a perturbation of the inverse mass matrix. And we have two new terms not present in the unperturbed form. One is a quadratic form in ρ and stems from transforming H_0 ; the other one is the time derivative (58) of the generating function.

The first error is the more difficult one to estimate. For small values of ζ the eigenvalues of the Hermitian matrix $(f_\xi^t f_\xi)^{-1}$ should hardly change according to Theorems by Hoffman–Wielandt and Weyl, respectively [31]. Thus we may neglect the perturbation of the equation for $\dot{\xi}$. The influence on the equation for $\dot{\pi}$ depends on how ξ enters this matrix. We will see later that in the case of the pendulum the matrix does not depend on ξ and thus no perturbation of this equation occurs.

The second error corresponds to what Alishenas [1, 2] called the *extra error*. It may be considered as an perturbation of the potential V due to the drift. Most of the extra error vanishes, if the residual ρ of the momentum constraints $\psi = 0$ is kept zero. This result confirms Alishenas' observation that, in general, numerical calculations are very sensitive to errors in the momenta (or velocities in the Lagrangian approach). On the other hand the momenta are especially affected by the extra error. The matrix $(\phi_q \phi_q^t)^{-1}$ of the quadratic form depends only on ξ and not on π . Thus it generates additional terms only in the equations of motion for π .

The terms generating the extra error may schematically be decomposed into three bilinear forms $\rho^t A_1 \rho + \zeta^t A_2 \rho + \zeta^t A_3 \pi$ with some matrices A_1, A_2, A_3 . If we neglect again the dependency of these matrices on ζ , we can get further information about the behavior of the error. We showed in the last section that ζ, ρ grow linearly in time, as $\dot{\zeta}$ is bound by a constant. At the beginning of a numerical integration the constraint residuals are still very small. Therefore the linear term $\zeta^t A_2 \rho$ dominates the quadratic term $\rho^t A_1 \rho$. Alishenas called this the normal phase of the integration. As the residuals grow, the influence of the quadratic term becomes stronger leading to a quadratic growth of the extra error. In this phase the numerical results become rapidly useless.

The importance of the momentum constraints $\psi = 0$ is easily understood geometrically. They represent a tangency condition for the position constraints $\phi = 0$. Their preservation leads thus also to a stabilization of the position constraints. But conversely, the preservation of $\phi = 0$ yields no feedback on the momentum constraint residuals, as it does not affect the momentum variables.

For the extended Hamiltonian we can use the same approach; this time based on (54). A perturbed Hamiltonian state space form is obtained by applying the symplectic mapping $_{\zeta, \rho}$ to H_e and computing the corresponding Hamiltonian equations of motion with the Poisson bracket (51). In general, this state space form coincide with (57) only for $\zeta = \rho = 0$. Again a general analysis is not possible, as the transformed Hamiltonian \tilde{H}_e depends on the precise form of the multipliers.

Finally, one should note that it is of course also possible to consider the equations (53) as a coordinate transformation in the full phase space. Applying this change of coordinates directly to the equations of motion leads to a system of differential equations not only for (ξ, π) but also for (ζ, ρ) . In the latter variables this system is, however, not necessarily Hamiltonian. Thus we have not fully achieved the canonical transformation used at the beginning of the last section. Furthermore, this way we miss the contribution of the time derivative (58) of the generating function which can be quite important.

10. THE PENDULUM REVISITED I: STABILITY

We apply now this stability analysis to the pendulum. This will enable us to give at least partial explanations for some of the numerical results shown in Figs. 1 and 2. We start with part (A). For the Hamilton-Dirac equations it was already

completely treated in Section 8. Theory and experiment both yield a linear growth of the constraint residuals and the energy error.

The differential equations (46) for the constraint residuals of the naive formulation are $\dot{\phi} = \psi$ and $\dot{\psi} = 0$. The origin is unstable for this system; thus it does not surprise that this approach yields the worst results. If we assume as in Section 8 that the perturbations introduced by the numerical errors are bounded by a constant in the considered time interval, we find in agreement with the experimental results in Section 6 that the momentum constraint residual grows linearly and the position constraint residual quadratically.

The analysis of the equations derived with the extended Hamiltonian is slightly more complicated. Computing $\dot{\phi}$ and $\dot{\psi}$ yields lengthy expressions in the phase space variables x, y, p_x, p_y . There exist different possibilities to eliminate these at least partially by introducing the constraints ϕ, ψ . In general, one even obtains a nonlinear form for (46). However, after linearization all these different forms lead to the same stability results. One possible form is obtained by applying (50)

$$(59) \quad \dot{\phi} = \frac{2\psi}{x^2 + y^2}\phi - \psi, \quad \dot{\psi} = \frac{4(p_x^2 + p_y^2) - y}{x^2 + y^2}\phi - \frac{2\psi}{x^2 + y^2}\psi.$$

A linearization of (59) yields $\dot{\phi} = -\psi$ and $\dot{\psi} = \frac{4(p_x^2 + p_y^2) - y}{x^2 + y^2}\phi$. For our initial data it follows from a simple energy consideration that the coefficient in the second equation is positive and the origin is thus a center.

This fact might explain why the curves for the extended Hamiltonian in Figs. 1 and 2 show such strong oscillations compared with the other two formulations. The effect of a perturbation of (59) is difficult to compute exactly. But adding a bounded perturbation to the linearized form of (59) with the coefficient treated as a constant does not lead to a growth of the residuals. Indeed in Fig. 2 the constraint residuals for the extended Hamiltonian grow significantly slower than for the Hamilton-Dirac equations. They are approximately proportional to \sqrt{t} .

In order to derive the perturbed Hamiltonian state space form introduced in Section 9 for part (B) of the stability analysis we need the symplectic mapping ζ, ρ defined by (53). It takes here the form

$$(60) \quad \begin{aligned} x &= \sqrt{2\zeta + 1} \sin \xi, & y &= \sqrt{2\zeta + 1} \cos \xi, \\ p_x &= \frac{\rho \sin \xi + \pi \cos \xi}{\sqrt{2\zeta + 1}}, & p_y &= \frac{\rho \cos \xi - \pi \sin \xi}{\sqrt{2\zeta + 1}}. \end{aligned}$$

Obviously, it yields indeed $\phi(x, y) = \zeta$ and $\psi(x, y, p_x, p_y) = \rho$.

Applying this mapping to the Hamiltonian H_0 yields

$$(61) \quad \tilde{H}_0 = \frac{1}{2} \frac{\pi^2}{2\zeta + 1} + \sqrt{2\zeta + 1} \cos \xi + \frac{1}{2} \frac{\rho^2}{2\zeta + 1}.$$

The time derivative of the generating function of ζ, ρ is given by

$$(62) \quad \frac{\partial S}{\partial t} = \dot{\zeta} \left[(1 - \cos 2\xi + \sin 2\xi)\pi + (1 + \cos 2\xi - \sin 2\xi)\rho \right].$$

We may now further analyze the stability of the Hamilton-Dirac equations for the pendulum by studying the equations of motion of the Hamiltonian $\tilde{H}_0 - \partial S / \partial t$. We have here the rather special case that in (61) neither the coefficient of π^2 nor the one of ρ^2 depends on ξ . Thus we get no perturbation of the equation for $\dot{\pi}$ from

these terms. The extra error stems here solely from the time derivative (62) of the generating function.

The perturbed Hamiltonian state space form is

$$(63) \quad \begin{aligned} \dot{\xi} &= \frac{1}{2\zeta + 1} \pi - \frac{\dot{\zeta}}{2} (1 - \cos 2\xi + \sin 2\xi), \\ \dot{\pi} &= \sqrt{2\zeta + 1} \sin \xi - \dot{\zeta} (\cos 2\xi + \sin 2\xi) (\rho - \pi). \end{aligned}$$

In both equations the second term stemming from (62) represent the extra error. Note that it has double the frequency of the pendulum.

The transformed extended Hamiltonian H_e is given by

$$(64) \quad \tilde{H}_e = \frac{1}{2} \frac{4\zeta + 1}{(2\zeta + 1)^2} \pi^2 + \frac{\zeta + 1}{\sqrt{2\zeta + 1}} \cos \xi - \frac{1}{2} \frac{\rho^2}{(2\zeta + 1)^2}.$$

It yields as a perturbed Hamiltonian state space form

$$(65) \quad \begin{aligned} \dot{\xi} &= \frac{4\zeta + 1}{(2\zeta + 1)^2} \pi - \frac{\dot{\zeta}}{2} (1 - \cos 2\xi + \sin 2\xi), \\ \dot{\pi} &= \frac{\zeta + 1}{\sqrt{2\zeta + 1}} \sin \xi - \dot{\zeta} (\cos 2\xi + \sin 2\xi) (\rho - \pi). \end{aligned}$$

In order to compare (63) and (65) we expand them in a power series in ζ . In (65) the first order terms vanish, thus a perturbation occurs only with ζ^2 . However, this advantage of the extended Hamiltonian gets probably more than compensated by the extra error, i. e. the terms stemming from (62). Although they are equal for both formulations, $\dot{\zeta}$ is considerably larger for the extended Hamiltonian due to the above mentioned oscillations of the constraint residuals. The same argument explains the smaller energy error of the Hamilton-Dirac equations. Besides (62) one must here also take into account the contribution of the third term in (61) and (64), respectively. But ρ is significantly smaller for the Hamilton-Dirac equations.

The behavior for inconsistent initial data is also interesting. As discussed in Section 8, the Hamilton-Dirac equations know nothing about the true constraint manifold: if the initial data lie on the submanifold $\mathcal{M}_{\zeta, \rho}$ defined by $\phi = \zeta$ and $\psi = \rho$ for some constants ζ, ρ , the exact solution for these initial values remains on $\mathcal{M}_{\zeta, \rho}$ and the numerical solution shows the same behavior with respect to $\mathcal{M}_{\zeta, \rho}$ as with respect to the true constraint manifold $\mathcal{M}_{0,0}$ in the case of consistent initial values. In the formulation with the extended Hamiltonian the trajectory always tries to reach $\mathcal{M}_{0,0}$ but actually oscillates around it.

11. THE PENDULUM REVISITED II: PROJECTIONS

Since all formulations still show a drift off the constraint manifold, one may want to add projections in order to enhance the preservation of the constraints. This is a standard approach to differential algebraic equations [15]. We consider again systems with a separable Hamiltonian $H_0 = \frac{1}{2} p^t p + V(q)$, imposed primary constraints $\phi(q) = 0$ and secondary constraints $\psi(q, p) = \phi_q p = 0$. If \tilde{p} denotes the value of the momenta obtained after one integration step, we set

$$(66) \quad p = \tilde{p} - \phi_q^+ \phi_q \tilde{p}$$

where $\phi_q^+ = \phi_q^t (\phi_q \phi_q^t)^{-1}$ is the Moore-Penrose pseudo inverse of the constraint Jacobian. This corresponds to an orthogonal projection on the submanifold defined by the secondary constraints $\psi = 0$.

For the correction of the position coordinates we may use a Newton-Raphson scheme with a frozen matrix. This yields the following iteration, if \tilde{q} denotes the value obtained after one integration step

$$(67) \quad \phi_q(\tilde{q})\Delta q = \phi(q^{(k)}), \quad q^{(k+1)} = q^{(k)} - \Delta q, \quad q^{(0)} = \tilde{q}.$$

The under-determined system is again solved with the Moore-Penrose pseudo inverse and the iteration is stopped, as soon as $|\phi(q^{(k)})|$ is smaller than a given tolerance ϵ .

Applied to the pendulum we obtain for the momentum correction

$$(68) \quad \begin{pmatrix} p_x \\ p_y \end{pmatrix} = \begin{pmatrix} \tilde{p}_x \\ \tilde{p}_y \end{pmatrix} - \frac{x\tilde{p}_x + y\tilde{p}_y}{x^2 + y^2} \begin{pmatrix} x \\ y \end{pmatrix}.$$

Because of the simplicity of the constraints, it is actually easier not to use a frozen matrix in the position correction and the iteration takes the form

$$(69) \quad \begin{pmatrix} x^{(k+1)} \\ y^{(k+1)} \end{pmatrix} = \frac{1}{2} \left[1 + \frac{1}{(x^{(k)})^2 + (y^{(k)})^2} \right] \begin{pmatrix} x^{(k)} \\ y^{(k)} \end{pmatrix}.$$

In our numerical experiments we corrected only when the constraint residuals exceeded a given tolerance ϵ . The decision whether a correction is necessary was taken independently for the position and the momentum constraint. If both needed a correction, the projection on the position constraint was performed first, so that the momentum projection could already use the corrected position coordinates.

As expected from our stability considerations the Dirac bracket formulation needs always the least number of projections. The precise gain depends of course on the relation between the used step size and the given tolerance for the constraint residuals. Choosing for example $h = 0.1$ and $\epsilon = 10^{-6}$, one needs for the Hamilton-Dirac equations on average in every second integration step a projection. With the other two approaches one must perform projections almost every step. For smaller step size the difference is even larger.

The conjecture in Section 9 that preserving the momentum constraint is more important than preserving the position constraint was also confirmed. This could be seen best in the naive formulation where even the qualitative properties were improved by momentum corrections, whereas position corrections alone did not lead to any change in the qualitative behavior of the errors.

With a momentum projection one obtains the same result as for the Dirac bracket formulation: quadratic growth of the integration error, linear growth of the energy error. The smaller ϵ the more similar the behavior of both formulations becomes. This is easy to understand, if one compares the equations of motion (38) and (35) (or more generally (27) and (31)). They differ only in terms proportional to the momentum constraint function ψ . If this constraint is enforced by projections, one obtains essentially the same equations of motion.

Applied to the stabilized formulations the projections have also negative effects. This holds especially for the extended Hamiltonian, where the results become much worse. Although the qualitative behavior of the integration and the energy error does not change, their absolute values are larger than without projections. The Hamilton-Dirac equations also do not like position corrections, whereas they profit from momentum corrections. In contrast, the naive formulation always gains.

For the energy error this is not surprising, as the orthogonal projections do not conserve the energy. The same holds of course for other conservation laws if present. Thus it appears that projection methods must be used with care in applications

where conservation laws are important. Or one projects on the manifold defined by the conservation laws, too.

The cause of the higher integration error is unclear. Shampine [29] (see also [13]) proved that projections do not disturb the convergence of one-step methods and that the order of the methods remains unchanged. The proof indeed allows for higher errors. This is in marked contrast to the result of Eich [13, 14] that for multi-step methods projections even reduce the local error.

12. CONCLUSION

There are two basic strategies for dealing numerically with differential algebraic equations. One can modify the equations; this leads to stabilization and index reduction techniques. Or one designs special numerical schemes like projection methods. Obviously, these two strategies are complementary and can be combined. A large part of the current literature on differential algebraic equations follows the second strategy. We studied in this article mainly the first approach for the special case of constrained Hamiltonian systems.

There have been a few attempts to stabilize general differential algebraic equations [4]. However, no systematic solution with a solid theoretical foundation has emerged so far. A classical example for the problems encountered is the Baumgarte stabilization [5] where the choice of the parameters is to a large extent still a question of try and error.

In physical problems like Hamilton dynamics the arising differential equations possess special properties. In this article we exploited the symplectic structure of the phase space to derive a stable formulation of the equations of motion. The geometry behind this approach allowed us to demonstrate the stability not only in numerical experiments but also with theoretical considerations.

Recently, we [26] studied the stability properties of the Faddeev-Jackiw formalism, a first-order approach to constrained dynamics. We could show that an additional term appears in its equations of motion corresponding to a vector field normal to the constraint manifold and vanishing on it. Thus as soon as a drift off this manifold occurs, the trajectory is forced back.

This approach uses an extended phase space and also modifies the symplectic structure there. Restricted to the original phase space this modified structure coincides with the Dirac bracket. Nevertheless, the arising equations of motion differ from the Hamilton-Dirac equations. But numerical experiments showed that both approaches lead to almost identical results even for long integration intervals. This clearly indicates that the physical properties of the Dirac bracket are the cause of the observed stability.

For systems with a large number of constraints the efficiency of the Dirac bracket approach depends crucially on the matrix C which must be inverted at each evaluation of the Hamilton-Dirac equations. As the example of the chain molecule demonstrated, this inversion can be significantly simplified by exploiting special constraint structures like “nearest neighbors constraints.” Note that for the Hamilton-Dirac equations it suffices to invert numerically, whereas the extended Hamiltonian approach needs in addition derivatives of C^{-1} to set up the equations of motion.

Another important difference between the Hamilton-Dirac equations and the equations derived with the extended Hamiltonian is that for the former one the constraint functions become first integrals, whereas for the latter one they represent

only weak invariants. For a higher degree of constraint preservation one can thus use a special scheme for maintaining invariants. Moan [23] constructed recently explicit Runge-Kutta methods preserving quadratic first integrals. Among them is a second order method with three stages that applied to the chain molecule yields with less evaluations better results than the standard fourth order scheme.

Studying such special numerical schemes applied to the Hamilton-Dirac equations is the logical next step. Mechanical integrators like energy conserving or symplectic methods are of special interest in this context. We mentioned already some preliminary results in Section 7.

Finally, we note that Dirac brackets can be generalized to infinite-dimensional systems. Thus this approach could also be useful for problems in electrodynamics, continuum mechanics etc. like the impetus-striction formalism [8, 22].

REFERENCES

- [1] T. Alishenas, *Zur Numerischen Behandlung, Stabilisierung durch Projektion und Modellierung Mechanischer Systeme mit Nebenbedingungen und Invarianten*, Ph.D. thesis, Dept. of Numerical Analysis and Computer Science, Royal Institute of Technology, Stockholm, Sweden, 1992.
- [2] T. Alishenas and Ö. Ólafsson, *Modeling and velocity stabilization of constrained mechanical systems*, BIT **34** (1994), 455–483.
- [3] H.C. Andersen, *Rattle — a velocity version of the Shake algorithm for molecular dynamics calculations*, J. Comp. Phys. **52** (1983), 24–34.
- [4] U.M. Ascher, H. Chin, and S. Reich, *Stabilization of DAEs and invariant manifolds*, Num. Math. **67** (1994), 131–149.
- [5] J. Baumgarte, *Stabilization of constraints and integrals of motion in dynamical systems*, Comp. Meth. Appl. Mech. Eng. **1** (1972), 1–16.
- [6] K.E. Brenan, S.L. Campbell, and L.R. Petzold, *Numerical solution of initial-value problems in differential-algebraic equations*, Classics in Applied Mathematics 14, SIAM, Philadelphia, 1996.
- [7] G.J. Cooper, *Stability of Runge-Kutta methods for trajectory problems*, IMA J. Num. Anal. **7** (1987), 1–13.
- [8] D.J. Dichmann, J.H. Maddocks, and R.L. Pego, *Hamiltonian dynamics of an elastica and the stability of solitary waves*, Arch. Rat. Mech. Anal. **135** (1996), 357–396.
- [9] P.A.M. Dirac, *Generalized Hamiltonian dynamics*, Can. J. Math. **2** (1950), 129–148.
- [10] ———, *Generalized Hamiltonian dynamics*, Proc. Roy. Soc. A **246** (1958), 326–332.
- [11] ———, *Lectures on quantum mechanics*, Belfer Graduate School Monograph Series 3, Yeshiva University, New York, 1964.
- [12] G.V. Dunne, R. Jackiw, and C.A. Trugenberger, *Topological (Chern-Simons) quantum mechanics*, Phys. Rev. D (1990), 661–666.
- [13] E. Eich, *Projizierende Mehrschrittverfahren zur Numerischen Lösung von Bewegungsgleichungen Technischer Mehrkörpersysteme mit Zwangsbedingungen und Unstetigkeiten*, Fortschrittsberichte, Reihe 18, Nr. 109, VDI-Verlag, Düsseldorf, 1992.
- [14] ———, *Convergence results for a coordinate projection method applied to mechanical systems with algebraic constraints*, SIAM J. Num. Anal. **30** (1993), 1467–1482.
- [15] E. Eich, C. Führer, B. Leimkuhler, and S. Reich, *Stabilization and projection methods for multibody dynamics*, Research Report A281, Helsinki University of Technology, Institute of Mathematics, 1990.
- [16] H. Goldstein, *Classical mechanics*, Addison-Wesley, New York, 1980.
- [17] E. Hairer, *Backward analysis of numerical integrators and symplectic methods*, Ann. Num. Math. **1** (1994), 107–132.
- [18] M. Henneaux and C. Teitelboim, *Quantization of gauge systems*, Princeton University Press, 1992.
- [19] L.O. Jay, *Symplectic partitioned Runge-Kutta methods for constrained Hamiltonian systems*, SIAM J. Numer. Anal. **33** (1996), 368–387.

- [20] B.J. Leimkuhler and S. Reich, *Symplectic integration of constrained Hamiltonian systems*, Math. Comp. **63** (1994), 589–605.
- [21] B.J. Leimkuhler and R.D. Skeel, *Symplectic numerical integrators in constrained Hamiltonian systems*, J. Comp. Phys. **112** (1994), 117–125.
- [22] J.H. Maddocks and R.L. Pego, *An unconstrained Hamiltonian formulation for incompressible fluid flow*, Comm. Math. Phys. **170** (1995), 207–217.
- [23] P.C. Moan, *The numerical solution of ordinary differential equations with conservation laws*, Master's thesis, Norwegian Institute of Technology, Trondheim, 1996.
- [24] S. Reich, *Symplectic integration of constrained Hamiltonian systems by composition methods*, SIAM J. Num. Anal. **33** (1996), 475–491.
- [25] J.M. Sanz-Serna and M.P. Calvo, *Numerical Hamiltonian problems*, Applied Mathematics and Mathematical Computation **7**, Chapman&Hall, London, 1994.
- [26] W.M. Seiler, *Involution and constrained dynamics II: The Faddeev-Jackiw approach*, J. Phys. A **28** (1995), 7315–7331.
- [27] ———, *Numerical analysis of constrained Hamiltonian systems and the formal theory of differential equations*, Math. Comp. Simul. to appear (1997).
- [28] W.M. Seiler and R.W. Tucker, *Involution and constrained dynamics I: The Dirac approach*, J. Phys. A **28** (1995), 4431–4451.
- [29] L.F. Shampine, *Conservation laws and the numerical solution of ODEs*, Comp. Math. Appl. **12** (1986), 1287–1296.
- [30] J. Śniatycki, *Dirac brackets in geometric dynamics*, Ann. Inst. Henri Poincaré A **20** (1974), 365–372.
- [31] G.W. Stewart and J.G. Sun, *Matrix perturbation theory*, Academic Press, Boston, 1990.
- [32] K. Sundermeyer, *Constrained dynamics*, Lecture Notes in Physics 169, Springer-Verlag, New York, 1982.

INSTITUT FÜR ALGORITHMEN UND KOGNITIVE SYSTEME, UNIVERSITÄT KARLSRUHE, D-76128
KARLSRUHE, GERMANY

E-mail address: `werner.seiler@informatik.uni-karlsruhe.de`